



Long-wavelength tilting of the Australian continent since the Late Cretaceous

Lydia DiCaprio^{a,b,*}, Michael Gurnis^b, R. Dietmar Müller^a

^a School of Geosciences, The University of Sydney, Sydney, NSW 2006, Australia

^b Seismological Laboratory, California Institute of Technology, Pasadena, California, USA

ARTICLE INFO

Article history:

Received 22 December 2007

Received in revised form 2 November 2008

Accepted 22 November 2008

Available online 21 January 2009

Editor: R.D. van der Hilst

Keywords:

Australia

Cenozoic

topography

subduction

dynamic topography

global sea level

Australian Antarctic Discordance

paleo-shoreline

ABSTRACT

Global sea level and the pattern of marine inundation on the Australian continent are inconsistent. We quantify this inconsistency and show that it is partly due to a long wavelength, anomalous, downward tilting of the continent to the northeast by 300 m since the Eocene. This downward tilting occurred as Australia approached the subduction systems in South East Asia and is recorded by the progressive inundation of the northern margin of Australia. From the Oligocene to the Pliocene, the long wavelength trend of anomalous topography shows that the southern margin of Australia is characterized by relative subsidence. We quantify the anomalous topography of the Australian continent by computing the displacement needed to reconcile the interpreted pattern of marine incursion with a predicted topography in the presence of global sea level variations. On the southern margin, long wavelength subsidence was augmented by at least 250 m of shorter wavelength anomalous subsidence, consistent with the passage of the southern continental margin over a north–south elongated, 500 km wide, topographic anomaly approximately fixed with respect to the mantle. The present day reconstructed position of this depth anomaly is aligned with the Australian Antarctic Discordance and is consistent with the predicted passage of the Australian continent over a previously subducted slab. Both the long-wavelength continental tilting and smaller-scale paleo-topographic anomaly on the southern Australian margin may have been caused by subduction-generated dynamic topography. These new constraints on continental vertical motion are consistent with the hypothesis that mantle convection induced topography is of the same order of magnitude as global sea level change.

© 2008 Elsevier B.V. All rights reserved.

1. Introduction

The magnitude of long wavelength anomalous topography produced by mantle processes is uncertain. Several kilometers of anomalous ocean floor depth near subduction zones and the super-swells around Southern Africa and in the western Pacific are attributed to mantle processes (Gurnis, 1990, 1993; Gurnis et al., 1998, 2000; Conrad et al., 2004; Xie et al., 2006; Zhang and Pysklywec, 2006; Gaina and Müller, in press). On continents, up to a kilometer of anomalous topography is attributed to mantle processes (Hager et al., 1985; Mitrovica et al., 1989; Lithgow-Bertelloni and Gurnis, 1997; Gurnis et al., 1998; Pysklywec and Mitrovica, 1998; Conrad and Gurnis, 2003; Artemieva, 2007; Heine et al., in review). However, estimating the magnitude of dynamically driven topography using geodynamic models is controversial due to the sensitivity of model predictions to input parameters, especially mantle viscosity and the scaling between seismic anomalies and density (Thoraval and Richards, 1997; Cadec and Fleitout, 1999). In addition, it is often difficult to separate the signal that results from convective processes, which we refer to in this

paper as dynamic topography, from the component of topography that results from lithospheric processes (Wheeler and White, 2000).

The role of convective processes in producing surface vertical motions is still debated but has significant implications for our understanding of the evolution of continents and sea level through time. In particular, marine advance and retreat into continental interiors is highly susceptible to evolving buoyancy in the mantle if the topography produced by convective process is of a similar magnitude to global sea level fluctuations. However, in order to isolate topography resulting from convective processes we must be able to completely remove any local and regional tectonic contribution to topography such as the subsidence due to lithospheric stretching or mountain building from distal (Dyksterhuis and Müller, 2008) or proximal plate boundaries.

The Australian continent is a prime candidate for studying the magnitude of surface topography caused by convective processes; the Cenozoic was a period of relative tectonic quiescence for the Australian continent and many of the major onshore physiographic features present today also existed at the beginning of the Cenozoic (Langford et al., 1995). However, there are several events that we must consider including the uplift of the Flinders Ranges either since the Miocene (Quigley et al., 2007; Sandiford, 2007) or before the Eocene (Veevers, 1984), intraplate volcanism in east Australia (Knutson, 1989), uplift of the southeastern highlands (Langford et al., 1995; van

* Corresponding author. Seismological Laboratory, California Institute of Technology, Pasadena, California, USA. Tel.: +1 626 395 3825; fax: +1 626 564 0715.

E-mail address: lydia@gps.caltech.edu (L. DiCaprio).

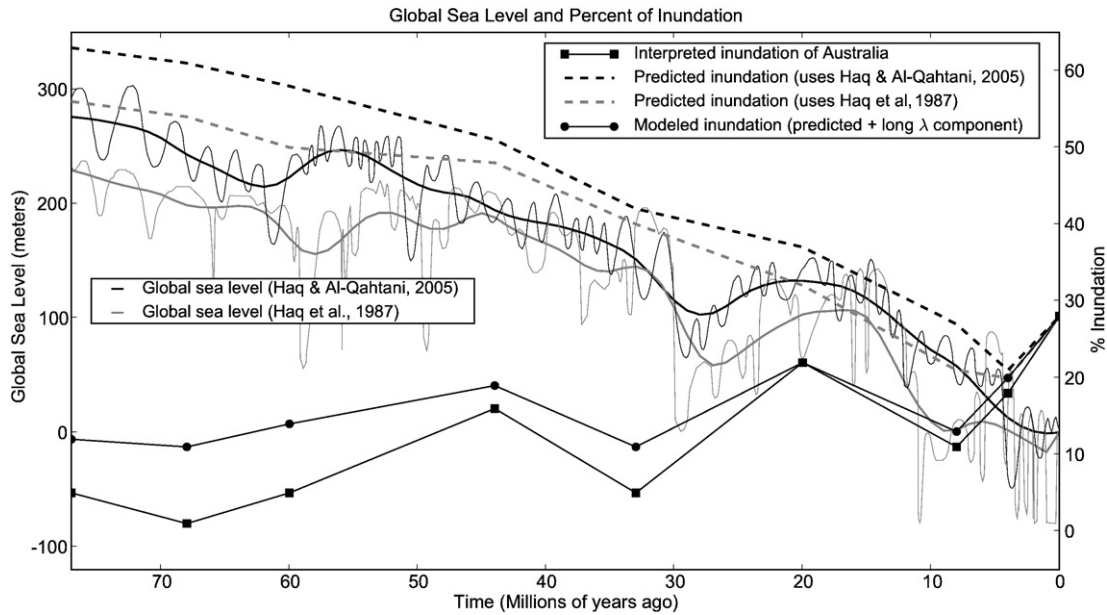


Fig. 1. Inundation history of Australia since the Late Cretaceous and percent flooding (right axis) and global sea level (left axis). The trend of the inundation history of the Australian continent since the Late Cretaceous is positive while the trend of global sea level is negative. Sediment removed model with global sea level (broken lines) and modeled inundation with long wavelength anomalous topography of the continent (right axis thick black line). Global sea level curves (thin black line, Haq and Al-Qahtani, 2005, thin gray line, Haq et al., 1987) are filtered using a cosine arch filter with 10 Myr window (thick black and grey lines). Total continental area is defined by the 200 meter isobath (ETOPO2 topography, (N.O.A.A., 2006). Time is defined at the midpoint of paleogeographic intervals (Langford et al., 1995).

der Beek et al., 2001), and post rift thermal subsidence along the northeastern margin (Langford et al., 1995; Müller et al., 2000c). However, during the Cenozoic, Australia was largely isolated from tectonic influence as the continent approached a region of subduction and putative long wavelength subsidence (Lithgow-Bertelloni and Gurnis, 1997). Consequently, Australia is an ideal continent from which to infer anomalous signals of long wavelength topography.

Despite the relative tectonic quiescence, the inundation of Australia is not consistent with global sea level fluctuations. Australia became progressively inundated throughout the Cenozoic despite a long-term fall in global sea level (Fig. 1). This was previously noted by several authors who proposed that the Australian continent was as much as 250 m higher at the beginning of the Cenozoic than it is today (Bond, 1978; Russell and Gurnis, 1994; Veevers, 1984, 2004). Lithgow-Bertelloni and Gurnis (1997) proposed the apparent subsidence since the Late Cretaceous may result from the motion of Australia toward subduction in Melanesia and Indonesia. Recently, Sandiford (2007) used the distribution of marine and non-marine sediments to show that the Australian continent experienced a topographic latitudinal asymmetry of marine inundation, since the Miocene. This involved tilting down towards the north, consistent with the continent approaching the dynamic topography low associated with the Melanesian subduction, north of Australia, and up in the southwest. Sandiford (2007) suggested that tilting up in the southwest progressively increased since the Neogene, related to the motion of the southern margin away from a putative dynamic topography low presently centered at the Australian Antarctic Discordance (AAD).

Here we investigate the long wavelength tilt of the Australian continent since the Late Cretaceous. After applying a global sea level curve (Haq et al., 1987; Haq and Al-Qahtani, 2005) to the sediment-load corrected topography, we isolate the topography that is the result of convective processes by comparing the predicted pattern of inundation with an interpreted pattern of marine inundation. We build on the work of Russell and Gurnis (1994) who proposed a bulk downward shift of the continent since the Cretaceous and Sandiford (2007) who proposed a continent wide, northward down tilt since the Neogene. We estimate the long wavelength anomalous topography with a planar surface and establish the magnitude of the evolving long

wavelength asymmetry of the Australian continent as a function of its northward motion towards the subduction systems of Melanesia and away from the evolving Australian Antarctic Discordance in the south. We use a planar surface since it is the simplest description of long wavelength anomalous topography that may be experienced continent wide. This method allows us to quantify the first order, long-wavelength effect of mantle convection on surface topography without the uncertainties associated with geodynamic models.

2. Methodology

We quantify the anomalous vertical motion of the Australian continent in three steps (Fig. 2). First, we interpret the position of the

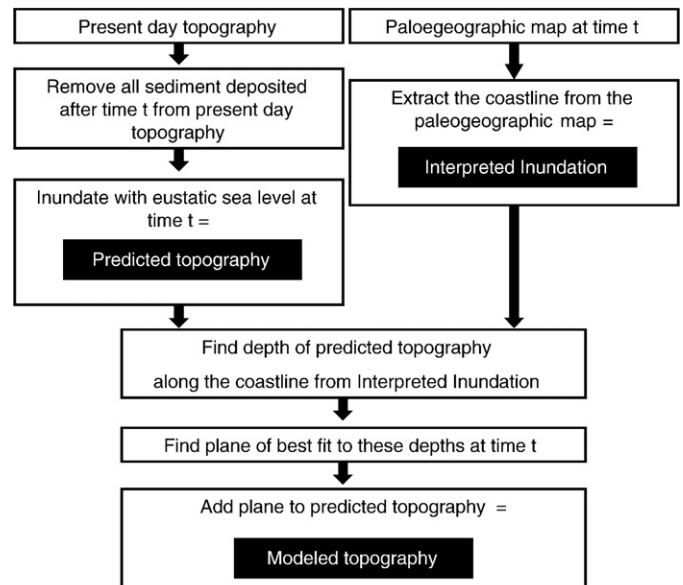


Fig. 2. Workflow for isolating the interpreted inundation, calculating the predicted topography and finding the modeled topography.

paleo-shoreline from published paleogeographic maps, here called interpreted inundation. Second, we calculate an expected pattern of inundation through time; We remove the effect of sediment loading from present day topography and adjust for global sea level, here called predicted topography. Third, we find a planar surface that minimizes the difference between the interpreted position of the paleo-shoreline and the predicted pattern of inundation; this planar surface quantifies the anomalous long wavelength topography, the sum of the predicted topography and the plane is referred to as modeled topography. We attempt to isolate and further quantify shorter wavelength deviations that are not captured by the long wavelength planar surface.

2.1. Interpreted inundation from paleo-shorelines

The extent of marine inundation (the paleo-shoreline), is inferred from the distribution of Late Cretaceous and Tertiary marine sediments preserved in outcrops and boreholes. We use paleogeographic maps of Australia (Langford et al., 1995) to define the paleo-shorelines. These maps are divided into time intervals ranging in length from 3 to 19.6 Myr between 80 Ma and 1.6 Ma. The paleogeographic maps are an interpretation of depositional environment (Struckmeyer and Brown, 1990) constrained by 361 data points, primarily bore holes that include lithology, unit thickness and depositional age (Fig. 3). We use the midpoint of each time interval as the reference time for comparing paleo-shorelines to modeled topography (time intervals are listed in online Supplementary Table S1).

2.2. Predicted topography

At each interval midpoint going back to the Late Cretaceous, we sequentially remove the sedimentary load from present day, 2 min gridded topography (N.O.A.A., 2006). The mass of the load is determined using lithology and compacted sediment thickness from well data. Sediments are decompacted and removed backward in time

using a one-dimensional backstripping methodology (see online Supplementary description S3 and Sclater and Christie (1980) for details of the backstripping methodology) according to common lithologic properties (see online Supplementary material S4). The change in the surface elevation of a point after the removal of sediment is given by an isostatic adjustment

$$\Delta H = z_s \frac{\rho_m - \bar{\rho}_s}{\rho_m - \rho_w} \quad (1)$$

Here z_s is the thickness of the decompacted sediment, ΔH is the equivalent column of air or water that is left after sediment removal, ρ_w is the density of material infilling the topographic depression (water or air), ρ_s is the average sediment density, and ρ_m is mantle density.

In order to remove the sediment from the entire continent we spatially interpolate ΔH between individual wells. Wells are irregularly spaced over Australia (Fig. 3) and originate from a variety of sources including those published in the paleogeographic atlas (Langford et al., 1995) and several from the Murray Basin adapted from Gallagher and Gourley (2007) and Müller et al. (2000b) (Fig. 3). For interpolation of the data onto a grid covering the entire continent we used minimum curvature surface fitting (Smith and Wessel, 1990). From Eq. (1), one can see that ΔH is a function of both sediment thickness and lithology. By interpolating the ΔH correction and not sediment thickness we preserve consistency between these two variables. In order to produce topography with the sediment removed we apply the interpolated grid of ΔH corrections to present day topography.

We avoid biasing the interpolation of well data by separating the data into land and marine groups and preventing interpolation into areas inferred to be erosional. As can be seen in Fig. 3, well data are more abundant offshore; by separately gridding the submarine and subaerial units, we avoid interpolation of the typically thicker and denser marine sediment onto land. No attempt to quantify the unloading of the

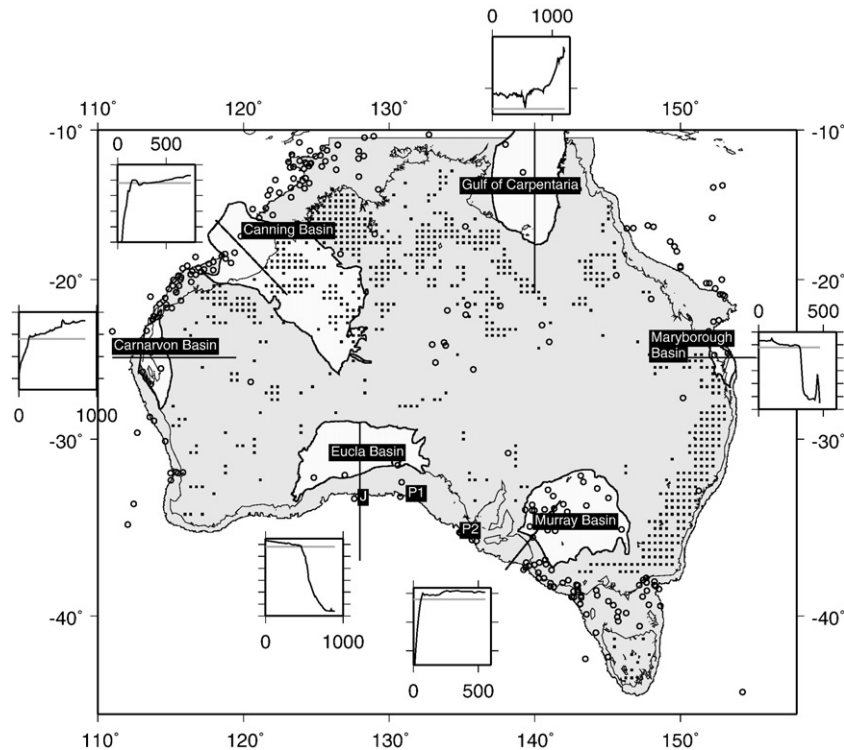


Fig. 3. The location of data used in this study. Boreholes (indicated with circles) and erosional areas (with squares). Six basins are selected (white). Inset plots show a profile (black line) with the shelf break at 200 m depth (grey line). Vertical tick marks are at 1000 m intervals in each profile. The extent of the 200 m isobath is shaded grey. Backstripped wells indicated as J1 for Jerboa 1 well, P1 for Potoroo well and P2 for Platypus.

continent due to erosion is made in this study due to the inherent difficulties in quantifying the amount of erosion and reconstructing eroded areas. However, our estimates of paleotopography are considered minima since topography would increase by about 200 m for every kilometer of restored erosion.

The predicted pattern of inundation is produced by removing sediment from the continent and then adjusting sea level according to published global sea level curves (Haq et al., 1987; Haq and Al-Qahtani, 2005). Both global sea level curves and the published well data use different absolute age scales. More recent age scales use updated biostratigraphic or radiometric information; however, the error within a particular age scale, covering times since the Late Cretaceous, is generally not more than 1 Myr (Rohde, 2003). At the midpoint of each paleogeographic the paleo-shoreline represents an average shoreline. The sediment corrections are made at these time midpoints and the average global sea level is taken for each paleogeographic interval. Since these intervals range in length from ~3 to 20 Myr, the error associated with timescale inconsistencies is insignificant.

2.3. Quantified anomalous topography as a plane

We are interested in the difference between the predicted topography and the interpreted inundation from paleo-shorelines. Since the topography at the shoreline is by definition zero meters above sea level the deviation of the predicted topography at the paleo-shoreline describes the anomalous displacement the continent has undergone. We assume the displacement is a long wavelength phenomenon such that the entire motion of the continent can be described by the tilting and uniform shift of a rigid plane. This is the simplest approximation to the displacement which captures a continent scale motion.

For every time interval described by the paleogeographic data we use a least squares inversion $m^{\text{est}} = \text{inv}(G'G)G'd$ to find the best fitting displacement plane $Gm=d$ where the data vector d is the predicted topography at the paleo-shoreline, m is a vector of model parameters which describes the plane (tilt to the north, tilt to the east and vertical offset), G is the design matrix that describes the relationship between m and d . (Parameters used to calculate the plane are listed in online Supplementary Table S2).

Since the paleogeographic maps are interpretations of depositional environment they include errors in the positioning of the paleo-shoreline. Langford et al. (1995) consider data points to be within 5 km of their true position but do not state the accuracy of the interpreted features. An effort to fully analyze the magnitude of any errors in interpreted paleo-shoreline positioning is beyond the scope of this paper. However, in order to minimize interpretative errors from the paleogeographic maps we include only the predicted topography data (i.e. topography with sediment removed and inundated with sea level) sampled from a shoreline, which lies within the area defined by the 200 m isobath. The 200 m isobath generally defines the depth of the Australian shelf break (Struckmeyer and Brown, 1990) (Fig. 3). When the paleo-shoreline extends beyond the present day continental shelf we do not consider this to be reliable and exclude these regions when fitting the planar surfaces.

The northeastern marginal plateaus represent extended continental crust that experienced post rift subsidence following seafloor spreading in the Tasman and Coral Seas 90 to 52 Ma, (Gaina et al., 1999). The northeastern margin paleo-shoreline extended beyond present day continental shelf before the Late Oligocene. Consequently, all data points along the NE marginal shoreline before the Late Oligocene are excluded when estimating the predicted topography at the paleo-shoreline.

2.4. Plane error estimation

We find the planar surface which best fits the data using least squares regression. However, in order to quantify how well our planar

surface fits the data we manually adjust the north–south (m_2) and east–west (m_3) components of the least squares planar surface until we observe a qualitatively unacceptable amount and pattern of inundation. We qualitatively compare the paleogeographic maps to the resulting topography and consider the distance of paleo-shoreline mismatch, the total percentage of inundation and the likelihood of the resulting topographic relief (see online Supplementary material S6 for our decisions). A similar qualitative method was applied to Australian data for the Cretaceous (Russell and Gurnis, 1994). Fig. 4 shows m_2 and m_3 as a function of age along with the estimated acceptable range of adjustments to the plane; the range of possible adjustments to m_2 and m_3 is small but this range increases with increasing age indicating there are more significant paleo-shoreline uncertainties within the Cretaceous paleogeographic maps and/or a planar tilt is not an optimal tool to approximate Cretaceous anomalous topography.

3. Results comparing modeled inundation to interpreted Inundation

We add the calculated plane of best fit which approximates anomalous topography to the predicted topography and produce a modeled topography. Our modeled percent of inundation closely approximates the trend and magnitude of the interpreted percent of continental inundation taken from paleogeographic maps (Fig. 1). In both cases, the continent became progressively more inundated since the Late Cretaceous. In contrast, the inundation predicted by sediment unloading and global sea level alone (i.e. without the added planar tilt), is one of progressive exposure since the Late Cretaceous (Fig. 1).

3.1. Late Cretaceous results

During the Late Cretaceous, the modeled inundation is greater (12% to 19%) than the interpreted inundation (7% to 19%) (83 Ma to 52 Ma Fig. 5). This difference is largely due to mismatches along the southern margin (Fig. 5B and C).

3.2. Tertiary results

Modeled inundation is only slightly higher (0 to 4%) than interpreted inundation during the Tertiary (52 Ma to 2 Ma Fig. 5). During the Tertiary, the northern (Gulf of Carpentaria), northwestern

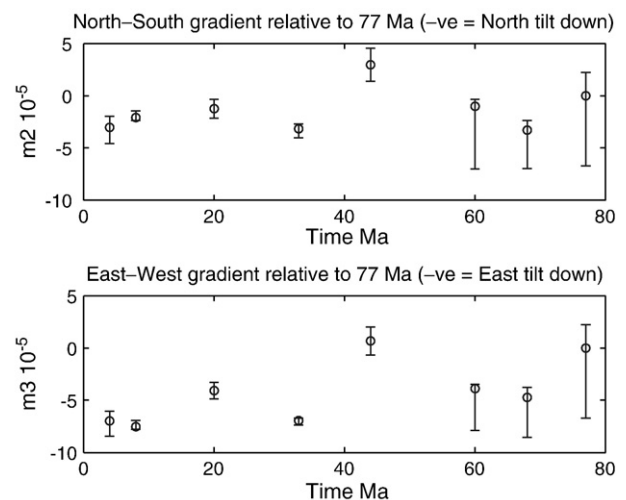


Fig. 4. The least squares solution of the latitudinal (m_2) and longitudinal (m_3) gradients which describe the inferred bi-linear tilt of the Australian continent. The error bounds are estimated by adjusting the minimum and maximum tilt of the bi-linear surface before an unacceptable amount of inundation or exposure is observed (maps showing these decisions are presented online as Supplementary material S6). Both plots show that the error is small and increases with increasing age.

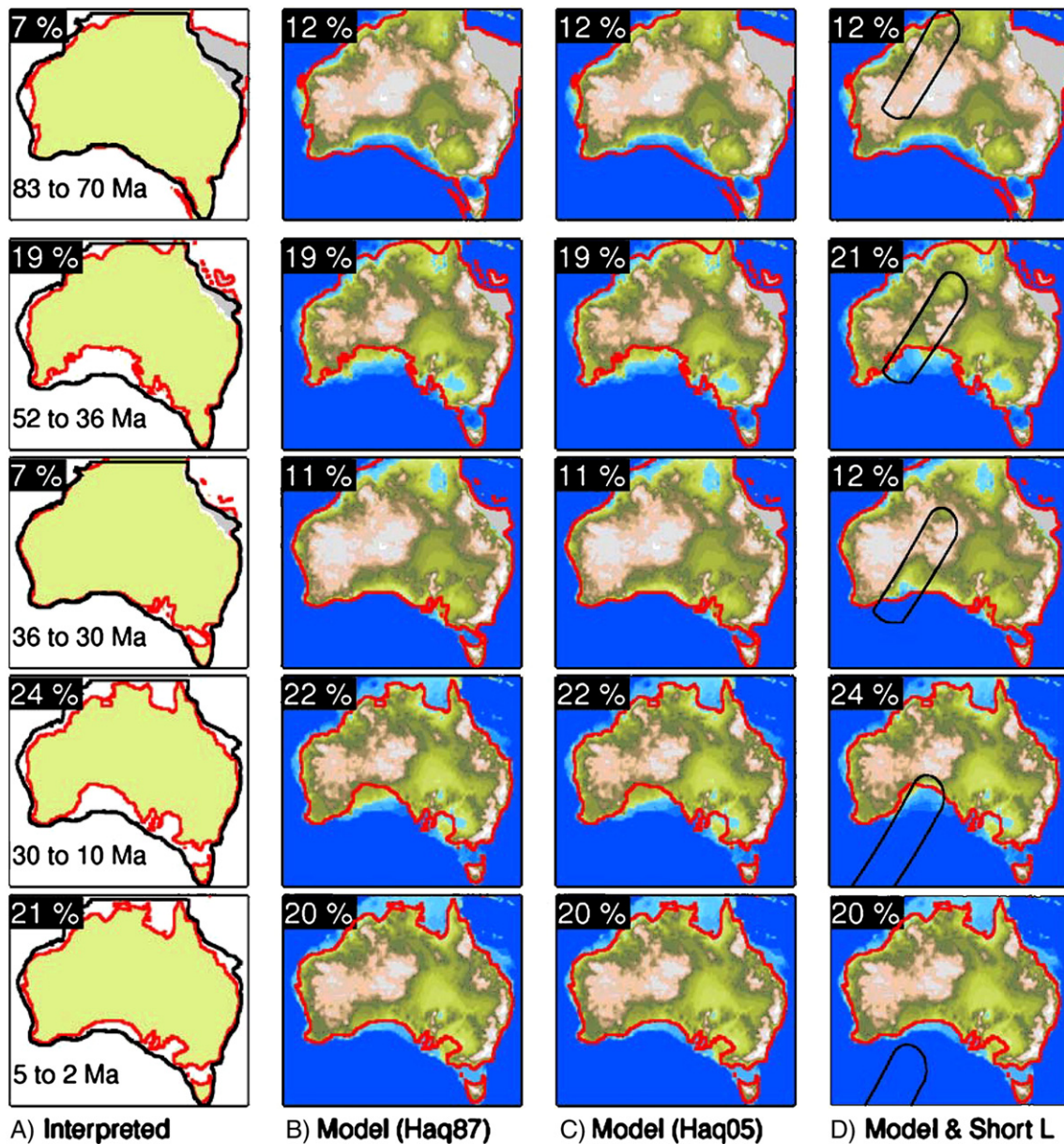


Fig. 5. Paleo-shoreline (A) and modeled inundation (B–D). We used Haq et al. (1987) (B) and Haq and Al-Qahtani (2005) (C) to calculate the long wavelength adjustment and compare the modeled topography to the marine inundation of Australia (A, shaded green and outlined in red). The present day 200 m isobath is plotted in black in A. The percent continental inundation for each case is shown at the top right corner. The area occupied by the northeastern marginal plateaus (shaded grey B, C, D) is removed from the calculated percent inundation. A short wavelength anomaly (D black outline) corrects the southern margin when it is added to the long wavelength tilt.

(Canning Basin), western (Carnarvon Basin) and eastern margins (Maryborough Basin) of Australia are well predicted by the modeled topography (Fig. 6). Despite the trend of falling sea level since the Neogene, this modeled inundation closely approximates the interpreted inundation on these margins and in particular exhibits the progressive inundation of the northern margin since the Oligocene.

3.3. The Tertiary Southern margin

Modeled topography closely fits the northern, western and northwestern margin paleo-shorelines. This suggests that a single long wavelength adjustment to predicted topography successfully accounts for the inundation pattern of the Australian continent during the Tertiary. However, along parts of the southern margin, the mismatch between modeled topography and paleoshorelines is significant. We propose this mismatch is accounted for by a shorter wavelength component of anomalous topography.

There are two principal areas of significant mismatch on the southern margin observed between modeled inundation and the paleo-shoreline. These two areas include the Eucla Basin located on the southern margin of Australia (Fig. 3) and the southeastern corner of Australia including the Murray Basin and Bass Strait between the Australian continent and Tasmania. As previously suggested (Sandiford, 2007), the record of inundation along the southern margin varies from east to west between these two regions. Fundamentally, our inundation mismatch indicates the southern margin is not explained by adding a planar adjustment to predicted topography.

Firstly, the modeled inundation for southeastern corner of Australia cannot explain the observed complete exposure of the Bass Strait and Murray Basin during the Eocene (52 to 36 Ma Fig. 5A). The modeled inundation is also unable to explain the progressive inundation of the Murray Basin from the Neogene until the Pliocene (30 Ma to 5 Ma Fig. 5A) (Langford et al., 1995; Sandiford, 2007) which was followed by a rapid and progressive period of off-lap. To match

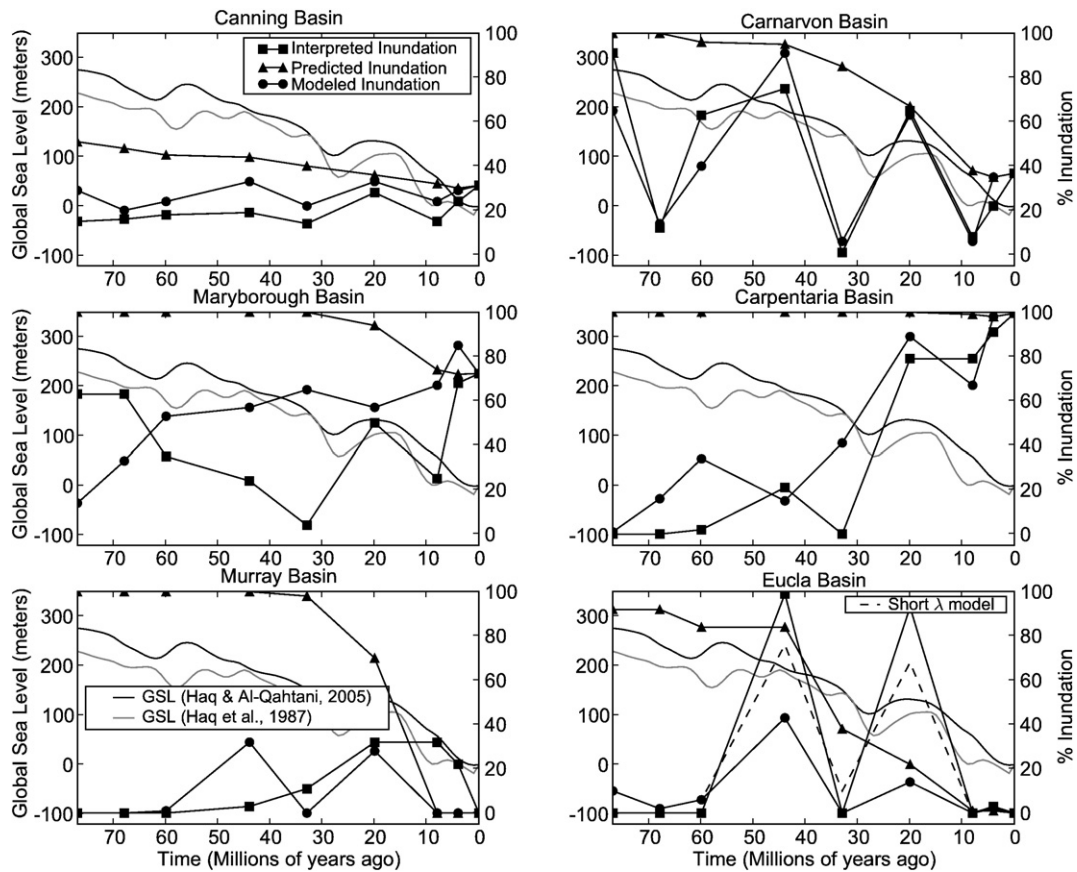


Fig. 6. A comparison between the interpreted inundation for selected basins on the continental margin and the modeled inundation. Two filtered global sea level curves (Haq et al., 1987; Haq and Al-Qahtani, 2005) are plotted on the left axis, the interpreted inundation, predicted inundation and modeled inundation is plotted on the right axis. The Eucla Basin includes an additional short wavelength component which closely matches the magnitude of interpreted inundation. Note also that in every case the modeled inundation matches the interpreted inundation better than the predicted inundation.

paleoshorelines in the southeastern corner of Australia, our model requires a further localized uplift in the Eocene followed by localized subsidence during the Tertiary until the Pliocene.

The inundation record of the Murray Basin is unique and local tectonics may provide an explanation for the inundation of this area. The subsidence and uplift history of the Murray Basin may be related to active faulting and uplift in the Southeastern Highlands (Jones and Veevers, 1982), which commenced at least as early as the Neogene (Sandiford, 2003), with faulting extending into the Murray Basin (Dickinson et al., 2002). At about six million years ago, the Murray basin experienced up to 180 m of inundation (Sandiford, 2007) and is now largely above sea level. Uplift in the Ottway ranges may have reached a magnitude of 174 to 240 m (Sandiford, 2003) while fossilized beaches in southeast Australia have undergone regional uplift of 250 m (Wallace et al., 2005). These stranded beaches show that the rate of uplift accelerated during the Quaternary (Sprigg, 1979; Wallace et al., 2005). This region has undergone unique local tectonic deformation that is not captured by a continent wide long wavelength signal of anomalous topography and is not here attributed to a shorter wavelength mantle convective process.

Secondly, modeled inundation cannot explain the amount of flooding of the southern margin during the Eocene (compare modeled inundation B and C to A between 52 to 36 Ma Fig. 5). Furthermore, modeled inundation is unable to explain the extensive inundation of the southern margin during the Miocene (observed inundation 30 to 10 Ma Fig. 6) and complete exposure by the Late Miocene (10–0 Ma Fig. 5A, observed inundation 10–0 Ma Fig. 6). To match paleoshorelines on the southern margin of Australia, our model requires an additional negative component of topography both during the Eocene and the Miocene.

The southern margin of Australia has a different inundation record from the Murray Basin and is too far from the southeastern highlands to have been influenced by these localized tectonics. The Eucla Basin contains a valuable relative sea level record which is preserved by Miocene and Eocene strandlines located some 400 km onshore. Sandiford (2007) suggested that this margin might be linked to the same process causing the AAD. The residual depth anomaly of the AAD, the Australian Antarctic Depth Anomaly (AADA), may be caused by a mantle source (Gurnis et al., 1998). Sandiford (2007) proposed that the southern margin was progressively uplifted since the Neogene while it moved away from a dynamic topography low associated with the AADA. It should be noted that following the Miocene inundation of the Eucla Basin the southern margin became exposed and this exposure is well matched by our modeled inundation (Fig. 5). Therefore, no additional short wavelength topographic component is required on the southern margin since the end of the Miocene.

4. The evolution of long wavelength anomalous topography

We find the position of the Australian continent relative to features thought to cause dynamic topography, (e.g. subduction zones), by rotating the continent relative to a moving hotspot absolute plate motion reference frame (O'Neill et al., 2003). The global plate motions are described by a collection of a number of relative plate motion models (Veevers, 1984; Royer and Sandwell, 1989; Royer and Chang, 1991; Veevers et al., 1991; Royer and Coffin, 1992; Royer and Rollet, 1997; Gaina et al., 1998; Tikku and Cande, 1999; Gaina et al., 1999; Müller et al., 2000a; Heine et al., 2004).

Referencing the long wavelength anomalous topography relative to 60 Ma (i.e. taking 60 Ma to have no tilt), shows the relative motion of the continent as it approached active subduction zones in Indonesia and Melanesia (Fig. 7). From the Paleocene until the Oligocene (60 to 33 Ma Fig. 7) the continent remains relatively flat with a slight upward tilt in the northeast. By the Oligocene the northeast of the continent tilted down by 100 m. This is coincident with the acceleration of spreading between Australian and Antarctica, which moved the northern margin of Australia towards the southwestward dipping subduction beneath the Melanesian arc. During the Miocene (20 Ma Fig. 7), the magnitude of this downward tilt increased to more than 200 m towards the north. From the Miocene until the Pliocene (8 to 4 Ma Fig. 7) the long wavelength tilt further increased to more than 300 m downward in the northeast as it approached the subduction systems to the east of Papua New Guinea. Progressive subsidence by more than 200 m is observed along the southern margin until the Pliocene (4 Ma Fig. 7). The subsidence along the southern margin indicates that in addition to the northeastward tilt of the continent, there was an overall bulk downward shift of the continent since the Paleocene.

The evolution of a broad northeastern downward tilt since the Eocene is coincident with the establishment of an extensive southeastward dipping subduction system beneath the Melanesian arc (Hall, 2002) and an increase in spreading rate between Antarctica and Australia (Whittaker et al., 2007). Subduction at the Greater Melanesian Arc was initiated around 43 Ma (Hall, 2002); it included the islands of New Britain, Bougainville, Vanuatu and the Solomon Islands (Kroenke, 1984) and may have been contiguous with subduction extending as far south as New Zealand (Hall, 2002: fig. 17).

The Miocene northward tilt (20 Ma Fig. 7) is contemporaneous with the collision along the northern margin of Australia with Papua New Guinea around 12 Ma (Hall, 2002). Loading and collision along this margin may account for the northward change in downward tilt at this time.

Referencing the long wavelength anomalous topography relative to 77 Ma shows the relative motion of the continent since the Late Cretaceous (Fig. 8). During the Late Cretaceous, the continent remained relatively flat until the Eocene (77 to 44 Ma Fig. 8). By the Eocene the whole continent was at least 100 m lower than during the Late Cretaceous. By the Miocene the entire Australian continent was more than 200 m lower than during the Late Cretaceous.

The relatively flat subsidence of the Australian continent during the Late Cretaceous is consistent with a period of little to no subduction near Australia. During the Late Cretaceous to the Paleocene the boundary between the Pacific and Australian plates was likely dominated by strike slip motion rather than subduction (Yan and Kroenke, 1993; Müller et al., 2000b). Our model for the Late Cretaceous is consistent with Russell and Gurnis (1994) who used Cretaceous inundation to show that the continent subsided in bulk with little tilting between 119 and 66 Ma. The overall bulk subsidence of the Australian continent since the Cretaceous is coincident with both the separation of India from Gondwanaland and the gradual drift of Australia away from Antarctica marking the breakup of Gondwanaland. The abundance of magmatism during the breakup of Gondwanaland (Storey et al., 1995) indicates that the mantle beneath the supercontinent may have been anomalously hot; the Cretaceous to Eocene bulk subsidence may be related to the movement of Australia away from this relatively hot mantle beneath Gondwanaland.

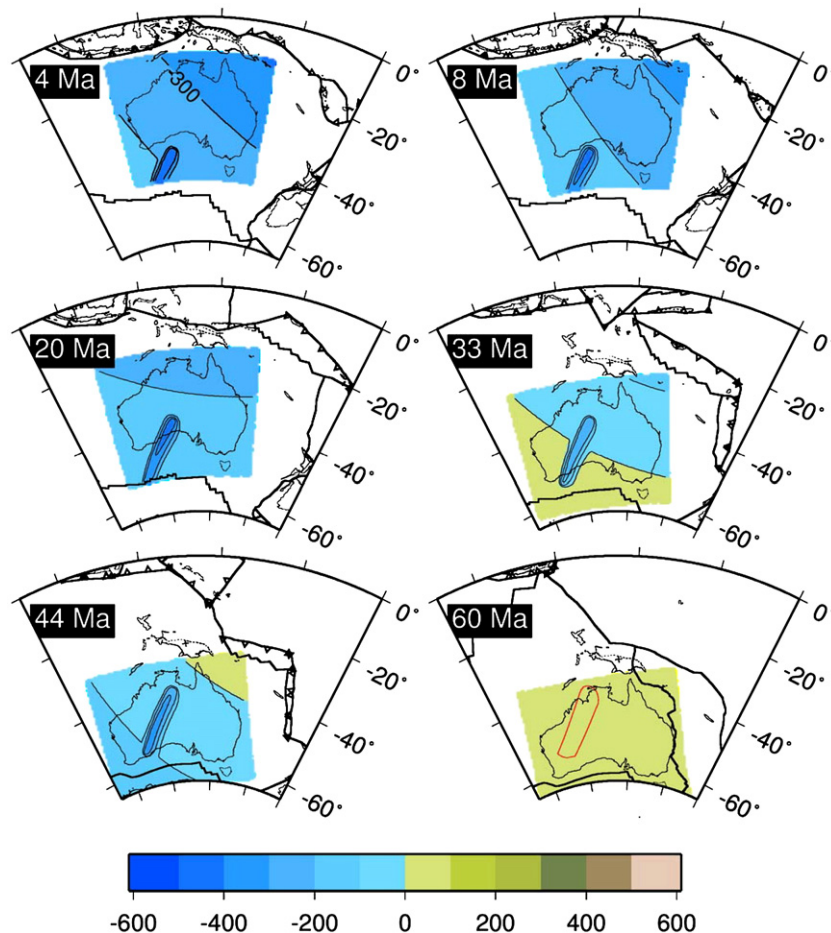


Fig. 7. Relative motion of the long wavelength anomalous topography of Australia since 60 Ma (with 100 m contours). The shorter wavelength anomalous topography is added to the long wavelength dynamic topography (red outline for times earlier than 60 Ma).

5. Short wavelength anomalous topography on the southern margin

In addition to long wavelength anomalous topography, a component of short wavelength anomalous topography is applied to make the southern margin modeled topography match the paleo-shorelines. This short wavelength feature is quantified and compared to the signal observed at the AAD. The magnitude and shape of the shorter wavelength anomalous subsidence is defined by examining the mismatch between modeled topography including the long wavelength tilt and a given paleo-shoreline. The shape of the anomaly is constrained according to the first appearance of anomalous subsidence recorded at wells offshore of the Eucla Basin. We exclude all data points from the southern margin before we compute the planar surface in order to completely isolate the short wavelength signal from the long wavelength tilting (Fig. 5D).

Previous studies of tectonic subsidence in the Great Australian Bight inferred accelerated subsidence in the Eocene, Oligocene and Miocene (Brown et al., 2001), which was attributed to accelerated spreading between Australia and Antarctica (Totterdell et al., 2000). We separate episodes of anomalous subsidence from post rift thermal subsidence using a lithospheric stretching model. We use the stretching factors estimated at

specific well locations based on seismic refraction data from Brown et al. (2003), based on an initial crustal thickness of 35 km (Brown et al., 2001) and vary the episode of rifting between 160 and 83 Ma (Totterdell et al., 2000) to match the rift subsidence recorded on the tectonic subsidence curve (Fig. 9) (properties used to calculate rift and post-rift subsidence are listed in the online Supplementary Table S5).

Maximum Eocene inundation on the southern margin occurred around 39 Ma (Sandiford, 2007) (52 to 36 Ma Fig. 5A) and a subsidence of between 150 and 250 m is required to match the modeled topography to the paleo-shoreline. Tectonic subsidence curves from wells offshore of the Eucla Basin show no anomalous subsidence at this time (Fig. 9). During the Miocene (30 to 10 Ma Fig. 5), additional subsidence of between 200 and 300 m is required to reconcile the paleo-shoreline to the modeled topography (Fig. 5D). Tectonic subsidence curves calculated from wells offshore of the Eucla Basin indicate up to 250 m of anomalous subsidence since the Miocene (Fig. 9). We create an anomaly with a gaussian shape in cross-section and a maximum amplitude of 250 m. We constrain the surface extent to permit the episodes of subsidence observed both onshore and offshore and fix this anomaly to the mantle.

Our modeled inundation with an additional short wavelength anomaly accounts for the inundation of the Eucla Basin in the Eocene

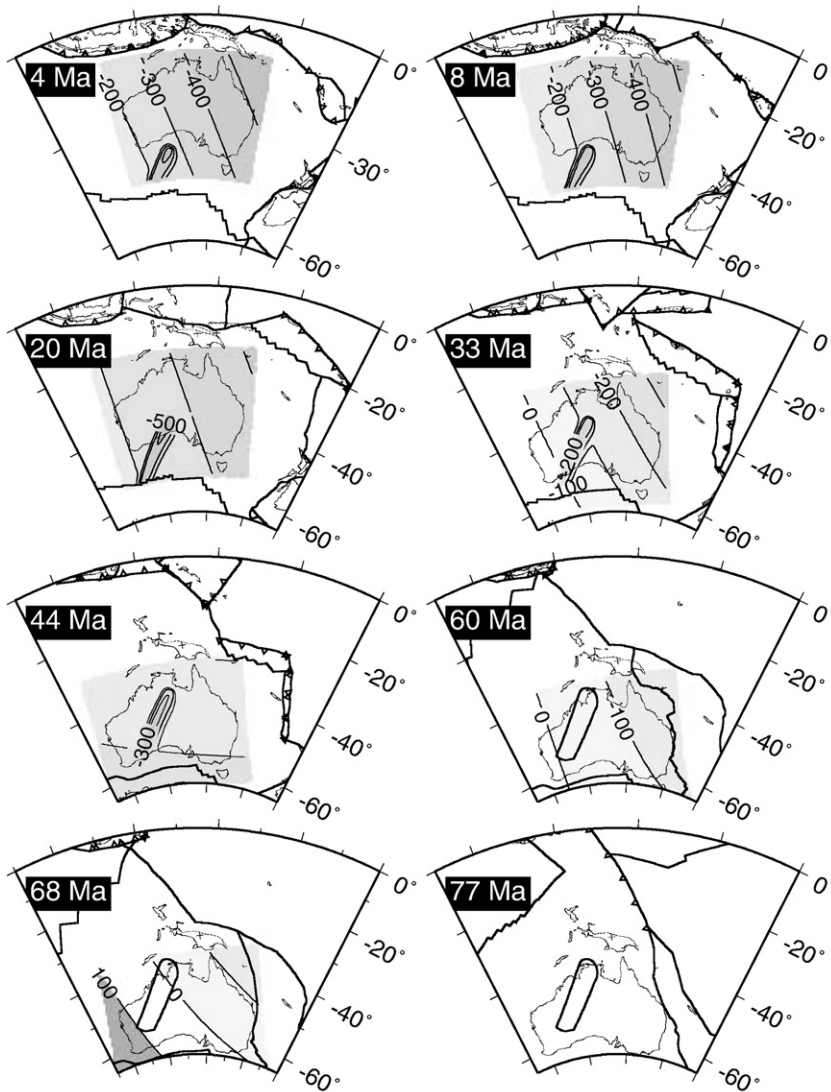


Fig. 8. Relative motion of the of the long wavelength anomalous topography of Australia since 77 Ma (with 100 m contours). The shorter wavelength anomalous topography is added to the long wavelength model. The long wavelength tilt from 77 Ma to 60 Ma is fairly flat with up to 100 m. By 4 Ma the long wavelength anomalous subsidence of the continent was between 200 and 500 m with a tilt down toward the east-northeast.

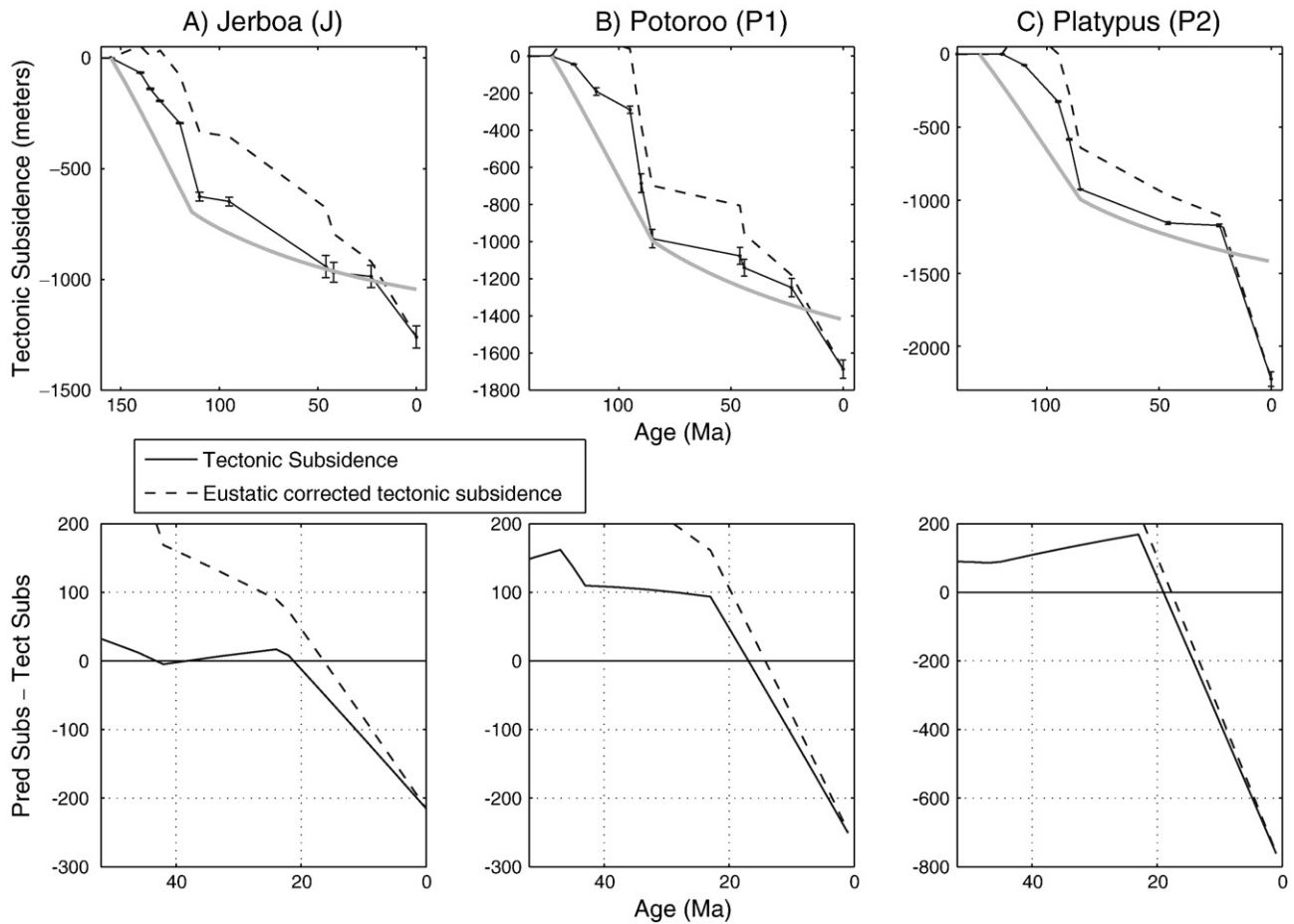


Fig. 9. Tectonic subsidence curves (thin black lines) from three wells offshore of the Eucla Basin with global sea level correction (dashed lines). Tectonic subsidence is subtracted from the predicted subsidence by rift and post-rift, thermal subsidence (grey) to show anomalous subsidence.

and the Miocene (at 44 Ma and 20 Ma, Figs. 5 and 6). During the Oligocene, (33 Ma, Fig. 6), the Eucla Basin experiences only a small increase in inundation due to the steeper gradient of the topography exposed at a time of low sea level.

The present day AADA correlates well with the reconstructed position of the proposed shorter wavelength anomalous topography (Fig. 7). Interestingly, the appearance of closely spaced fracture zones on the South East Indian Ridge associated with the Australian Antarctic Discordance correlates with the interception of the short wavelength anomaly with the spreading ridge in these reconstructions. Furthermore, the shorter wavelength anomaly lies in the same paleo position as earlier predictions for the passage of subducted material beneath the eastern margin of Australia, a model that also correctly predicts the present day location of the AAD (see Fig. 6D, E and F, Gurnis et al., 1998).

The shape of the proposed shorter wavelength anomaly does not account for the observed anomalous subsidence experienced at wells farther east, offshore of the Murray and Otway Basins. We do not yet have a complete understanding for the subsidence of these basins; however our observations provide an opportunity to explore the topographic evolution of the entire southern margin of Australia and the formation of the AADA with geodynamic models.

6. Conclusion

The vertical motion of the Australian continent since the Late Cretaceous is estimated using a planar surface to approximate the long wavelength dynamic topography of the Australian continent. Modeled inundation is a good first order approximation to interpreted paleo-shorelines especially on the northern, northwestern and western

margins. Calculating the relative vertical motion and rotating the long wavelength component of anomalous topography to its paleo position, shows that as the Australian continent approached subduction beneath Melanesia it was progressively pulled down in the northeast by as much as 300 m. From the Late Cretaceous until the Eocene, the Australian continent subsided by as much as 200 m but remained fairly flat relative to Late Cretaceous topography. Consequently, most of the north downward tilting post-dates the Early Eocene.

The Eucla Basin and Great Australian Bight have experienced long wavelength gradual subsidence punctuated by localized short wavelength subsidence. The cause for the short wavelength subsidence anomaly is most likely a temperature/compositional anomaly fixed relative to the mantle which was overridden by the Australian plate. The anomaly may indicate the source of the AAD since its reconstructed position correlates to the present day location of the AAD. Our models of vertical motion are likely to place strong constraints on a new generation of geodynamic models of the Australian region. Furthermore, our quantitative approach suggests that the magnitude of dynamic influences on topography may be of the same order of magnitude as sea level fluctuations and further modeling the dynamics of the Australian continent may confirm whether mantle anomalies can account for these topographic observations.

Acknowledgements

All figures except Figs. 2, 3 and 8 were generated using GMT (Wessel and Smith, 1991). We would like to thank Christian Heine who provided the basin outlines and the help and advice of Christopher DiCaprio. Lydia DiCaprio was funded by the Australian Research

Council Australian Postgraduate Award administered by the University of Sydney. This work represents contribution 8997 of the Division of Geological and Planetary Sciences, California Institute of Technology, and contribution 97 of the Tectonics Observatory. We thank M. Sandiford and an anonymous reviewer for their reviews that significantly improved this manuscript.

Appendix A. Supplementary data

Supplementary data associated with this article can be found, in the online version, at doi:10.1016/j.epsl.2008.11.030.

References

- Artemieva, I.M., 2007. Dynamic topography of the East European craton: shedding light upon lithospheric structure, composition and mantle dynamics. *Glob. Planet. Change* 58, 411–434.
- Bond, G.C., 1978. Speculations on real sea-level changes and vertical motions of continents at selected times in the Cretaceous and Tertiary Periods. *Geology* 6, 247–250.
- Brown, B., Müller, R.D., Struckmeyer, H.I.M., 2001. Anomalous tectonic subsidence of the southern Australian passive margin: response to Cretaceous dynamic topography or differential lithospheric stretching? In: Hill, K., Bernecker, T. (Eds.), *Eastern Australasian Basins 2001*, Volume Petroleum Exploration Society of Australia, Special Publ. The Australasian Institute of Mining and Metallurgy, Carlton, Victoria, pp. 563–569.
- Brown, B.J., Muller, R.D., Gaina, C., Struckmeyer, H.I.M., Stagg, H.M.J., Symonds, P.A., 2003. Formation and evolution of Australian passive margins: implications for locating the boundary between continental and oceanic crust. *Geological Society of Australia Special Publication*, pp. 223–243.
- Cadek, O., Fleitout, L., 1999. A global geoid model with imposed plate velocities and partial layering. *J. Geophys. Res.-Solid Earth* 104, 29055–29075.
- Conrad, C.P., Gurnis, M., 2003. Seismic tomography, surface uplift, and the breakup of Gondwanaland: integrating mantle convection backwards in time. *Geochem. Geophys. Geosyst.* 4(3), 1031.
- Conrad, C.P., Lithgow-Bertelloni, C., Loudon, K.E., 2004. Iceland, the Farallon slab, and dynamic topography of the North Atlantic. *Geology* 32, 177–180.
- Dickinson, J.A., Wallace, M.W., Holdgate, G.R., Gallagher, S.J., Thomas, L., 2002. Origin and timing of the Miocene–Pliocene unconformity in Southeast Australia. *J. Sediment. Res.* 72, 288–303.
- Dyksterhuis, S., Müller, D., 2008. Cause and evolution of intraplate orogeny in Australia. *Geology* 36, 495–498.
- Gaina, C., Müller, R.D., 2007. Cenozoic tectonic and depth/age evolution of the Indonesian gateway and associated back-arc basins: *Earth Science Reviews* 83, 177–203.
- Gaina, C., Müller, R.D., Royer, J.Y., Stock, J., Hardebeck, J., Symonds, P., 1998. The tectonic history of the Tasman Sea: a puzzle with 13 pieces. *J. Geophys. Res.* 103, 12413–12433.
- Gaina, C., Muller, R.D., Royer, J.Y., Symonds, P., 1999. Evolution of the Louisiade triple junction. *J. Geophys. Res.-Solid Earth* 104, 12927–12939.
- Gallagher, S.J., Gourley, T.L., 2007. Revised Oligo-Miocene stratigraphy of the Murray Basin, southeast Australia. *Aust. J. Earth Sci.* 54, 837–849.
- Gurnis, M., 1990. Bounds on global topography from Phanerozoic flooding of continental platforms. *Nature* 344, 754–756.
- Gurnis, M., 1993. Phanerozoic marine inundation of continents driven by dynamic topography above subducting slabs. *Nature* 364, 589–593.
- Gurnis, M., Müller, R.D., Moresi, L., 1998. Cretaceous vertical motion of Australia and the Australian–Antarctic discordance. *Science* 279, 1499–1504.
- Gurnis, M., Moresi, L., Muller, R.D., 2000. Models of mantle convection incorporating plate tectonics: the Australian region since the Cretaceous. In: Richards, M.A., Gordon, R., van der Hilst, R. (Eds.), *The History and Dynamics of Global Plate Motions*. Geophysical Monograph, vol. 121. American Geophysical Union, Washington D.C., pp. 211–238.
- Hager, H.B., Clayton, R.W., Richards, M.A., Comer, R.P., Dziewonski, A.M., 1985. Lower mantle heterogeneity, dynamic topography and the geoid. *Nature* 313, 541–545.
- Hall, R., 2002. Cenozoic geological and plate tectonic evolution of SE Asia and the SW Pacific: computer-based reconstructions, model and animations. *J. Asian Earth Sci.* 20, 353–431.
- Haq, B.U., Al-Qahtani, M., 2005. Phanerozoic cycles of sea-level change on the Arabian Platform. *GeoArabia* 10, 127–160.
- Haq, B.U., Hardenbol, J., Vail, P.R., 1987. Chronology of fluctuating sea levels since the Triassic. *Science* 235, 1156–1167.
- Heine, C., Müller, D., Gaina, C., 2004. Reconstructing the lost Eastern Tethys Ocean Basin: convergence history of the SE Asian margin and marine gateways. In: Clift, P.D., Hayes, D.E., Kuhnt, W., Wang, P. (Eds.), *Continent–Ocean Interactions within East Asian Marginal Seas*. Geophys. Monogr. Ser., vol. 149. American Geophysical Union, Washington, pp. 37–54.
- Heine, C., Müller, R.D., Steinberger, B., DiCaprio, L., in review. Integrating deep Earth dynamics in paleogeographic reconstructions of Australia: Paleoclimatology, Paleoclimatology.
- Jones, J.G., Veevers, J., 1982. A Cainozoic history of Australia's Southeast Highlands. *Aust. J. Earth Sci.* 29, 1–12.
- Knutson, J., 1989. East Australian Volcanic Geology. In: Johnson, R.W. (Ed.), *Intraplate Volcanism in Eastern Australia and New Zealand*. Press Syndicate of the University of Cambridge in association with the Australian Academy of Science, Cambridge, p. 408.
- Kronke, L., 1984. Solomons Islands: San Cristobal to Bougainville and Buka. In: Kronke, L. (Ed.), *Cenozoic Tectonic Development of the Southwest Pacific*. CCOP/SOPAC Tech. Bull., vol. 6. U.N. ESCAP, pp. 47–61.
- Langford, R.P., Wilford, G.E., Truswell, E.M., Isern, A.R., 1995. Palaeogeographic Atlas of Australia – Cainozoic, Cretaceous, vol. 10. Australian Geological Survey Organisation, Canberra.
- Lithgow-Bertelloni, C., Gurnis, M., 1997. Cenozoic subsidence and uplift of continents from time-varying dynamic topography. *Geology* 25, 735–738.
- Mitrovica, J.X., Beaumont, C., Jarvis, G.T., 1989. Tilting of the continental interiors by the dynamical effects of subduction. *Tectonics* 8, 1079–1094.
- Müller, R.D., Gaina, C., Clarke, S., 2000a. Seafloor spreading around Australia. In: Veevers, J. (Ed.), *Billion-year Earth History of Australia and Neighbours in Gondwanaland – BYEHA*. GEMOC Press, Sydney.
- Müller, R.D., Gaina, C., Tikku, A., Mihut, D., Cande, S., Stock, J.M., 2000b. Mesozoic/Cenozoic tectonic events around Australia. In: Richards, M., Gordon, R. (Eds.), *The History and Dynamics of Global Plate Motions*. American Geophysical Union Monograph, vol. 121. American Geophysical Union, pp. 161–188.
- Müller, R.D., Lim, V.S.L., Isern, A.R., 2000c. Late Tertiary tectonic subsidence on the northeast Australian passive margin: response to dynamic topography? *Mar. Geol.* 162, 337–352.
- N.O.A.A., 2006. In: Center, N.G.D. (Ed.), ETOPO2. U.S. Department of Commerce.
- O'Neill, C., Müller, R.D., Steinberger, B., 2003. Geodynamic implications of moving Indian Ocean hotspots. *Earth Planet. Sci. Lett.* 215, 151–168.
- Pysklywec, R.N., Mitrovica, J.X., 1998. Mantle flow mechanisms for the large-scale subsidence of continental interiors. *Geology* 26, 687–690.
- Quigley, M., Sandiford, M., Field, K., Alimanovic, A., 2007. Bedrock erosion and relief production in the northern Flinders Ranges, Australia. *Earth Surf. Process. Landf.* 32, 929–944.
- Rohde, R.A., 2003. In: Rohde, P.B.R.A. (Ed.), *GeoWhen*. International Commission on Stratigraphy.
- Royer, J.Y., Chang, T., 1991. Evidence for relative motions between the Indian and Australian plates during the last 20 m.y. from plate tectonic reconstructions: implications for the deformation of the Indo-Australian plate. *J. Geophys. Res.* 96, 11779–11802.
- Royer, J.Y., Coffin, M.F., 1992. Jurassic to Eocene plate tectonic reconstructions in the Kerguelen Plateau region. In: S.W. Wise, J., Julson, A.P., Schlich, R., Thomas, E. (Eds.), *Proceedings of the Ocean Drilling Program, Scientific Results*, vol. 120. Ocean Drilling Program, Texas A&M University, College Station, TX, pp. 917–930.
- Royer, J.Y., Rollet, N., 1997. Plate tectonic setting of the Tasmanian region. *Aust. J. Earth Sci.* 44, 543–560.
- Royer, J.Y., Sandwell, D.T., 1989. Evolution of the Eastern Indian Ocean since the Late Cretaceous: constraints from Geosat altimetry. *J. Geophys. Res.* 94, 13755–13782.
- Russell, M., Gurnis, M., 1994. The platform of epeirogeny: vertical motions of Australia during the Cretaceous. *Basin Res.* 6, 63–76.
- Sandiford, M., 2003. Neotectonics of southeastern Australia: linking the Quaternary faulting record with seismicity and in situ stress. In: Hillis, R.R., Müller, R.D. (Eds.), *Evolution and Dynamics of the Australian Plate*, vol. Special Publication 22. Geological Society of Australia, pp. 101–113.
- Sandiford, M., 2007. The tilting continent: a new constraint on the dynamic topographic field from Australia. *Earth Planet. Sci. Lett.* 261, 152–163.
- Slater, J.G., Christie, P.A.F., 1980. Continental Stretching – an explanation of the post Mid-Cretaceous subsidence of the Central Graben of the North Sea. *J. Geophys. Res.* 85, 3740–3750.
- Smith, W.H.F., Wessel, P., 1990. Gridding with continuous curvature splines in tension. *Geophysics* 55, 293–305.
- Sprigg, R.C., 1979. Stranded and submerged sea-beach systems of southeast south Australia and the aeolian desert cycle. *Sediment. Geol.* 22, 53–96.
- Storey, M., Mahoney, J.J., Saunders, A.D., Duncan, R.A., Kelley, S.P., Coffin, M.F., 1995. Timing of hot spot-related volcanism and the breakup of Madagascar and India. *Science* 267, 852–855.
- Struckmeyer, H.I.M., Brown, P.J., 1990. Australian Sea Level Curves Part 1: Australian Inundation Curves, Palaeogeography. Bureau of Mineral Resources, Geology and Geophysics Petroleum Division of the Australian Mineral Industries Research Association, GPO Box 378, Canberra, ACT 2601, Australia, pp. 1–55.
- Thoraval, C., Richards, M.A., 1997. The geoid constraint in global geodynamics: viscosity structure, mantle heterogeneity models and boundary conditions. *Geophys. J. Int.* 131, 1–8.
- Tikku, A.A., Cande, S.C., 1999. The oldest magnetic anomalies in the Australian–Antarctic Basin: are they isochrons? *J. Geophys. Res.* 104, 661–677.
- Totterdell, J.M., Blevin, J.E., Struckmeyer, H.I.M., Bradshaw, B.E., Colwell, J.B., Kennard, J.M., 2000. A new sequence framework for the great Australian Bight: starting with a clean slate. *APPEA J.* 95–117.
- van der Beek, P., Pulford, A., Braun, J., 2001. Cenozoic landscape development in the Blue Mountains (SE Australia): lithological and tectonic controls on rifted margin morphology. *J. Geol.* 109, 35–56.
- Veevers, J.J., 1984. *Phanerozoic Earth History of Australia*. Oxford University Press, New York. 418 pp.
- Veevers, J.J., 2004. Gondwanaland from 650–500 Ma assembly through 320 Ma merger in Pangea to 185–100 Ma breakup: supercontinental tectonics via stratigraphy and radiometric dating. *Earth-Sci. Rev.* 68, 1–132.
- Veevers, J.J., Powell, C.M., Roots, S.R., 1991. Review of seafloor spreading around Australia. I. Synthesis of the patterns of spreading. *Aust. J. Earth Sci.* 38, 373–389.
- Wallace, M.W., Dickinson, J.A., Moore, D.H., Sandiford, M., 2005. Late Neogene strandlines of southern Victoria: a unique record of eustasy and tectonics in southeast Australia. *Aust. J. Earth Sci.* 52, 279–297.

- Wessel, P., Smith, W.H.F., 1991. Free software helps map and display data. *EOS Trans. Am. Geophys. Union* 72, 441–446.
- Wheeler, P., White, N., 2000. Quest for dynamic topography: observations from Southeast Asia. *Geology* 28, 963–966.
- Whittaker, J., Müller, R.D., Leitchenkov, G., Stagg, H., Sdrolias, M., Gaina, C., Goncharov, A., 2007. Major Australian–Antarctic plate reorganization at Hawaiian–Emperor bend time. *Science* vol. 318.
- Xie, X., Müller, R.D., Li, S., Gong, Z., Steinberger, B., 2006. Origin of anomalous subsidence along the northern South China Sea Margin and its relationship to dynamic topography. *Mar. Pet. Geol.* 23, 745–765.
- Yan, C.Y., Kroenke, L.W., 1993. A plate tectonic reconstruction of the Southwest Pacific, 0–100 Ma. In: Berger, W.H., Kroenke, L.W., Mayer, L.A. (Eds.), *Proceedings of the Ocean Drilling Program, Scientific Results*, vol. 130, p. 697. Ocean Drilling Program, College Station, TX.
- Zhang, N., Pysklywec, R.N., 2006. Role of mantle flow at the North Fiji Basin: insights from anomalous topography. *Geochem. Geophys. Geosyst.* 7, 1–14.